THE **SMARTER APPROACH** TO UNDERSTAND STRUCTURE AND PROPERTIES OF NEW INORGANIC MATERIALS

Franck Fayon,

Mathieu Allix, Michael Pitcher, Cécile Genevois, Emmanuel Véron,

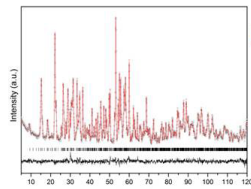P. Florian, V. Sarou-Kanian, A. Rakmatullin and D. Massiot

Orléans
France

SMARTER crystallography approach

Combining experimental characterization and simulation methods to solve complex structures

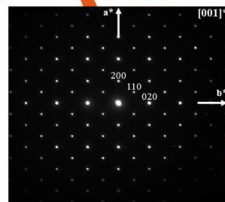**High-flux sources**
Rietveld (Bragg)
PDF (diffuse)

Powder Diffraction

⇒ **Average structural model**

SMARTER Crystallography

Structure

Elucidation

Structure determination by co**M**bining
m**A**gnetic **R**esonance, compu**T**ation
mod**E**ling and diff**R**actions

NMR Spectroscopy

^{11}B MAS

⇒ **Local state information**

Very high magnetic fields
28.2 T commercial !
Very fast sample spinning
120 kHz : 7 000 000 rd/min

A variety of correlation methods
Multinuclear, 2D, 3D, etc...

HR (S)TEM
(Sub)Atomic resolution
EELS
Precession e diffraction

TEM

⇒ **Symmetry / Nanometer scale**

DFT calculations

⇒ **Structure optimization/validation**

Ab initio computations
Structure prediction
DFT GIPAW & PAW → NMR

Diffraction is gold standard for inorganic materials but …..

2002 Chemistry Nobel : **Kurt Wüthrich** : 3D structure of biological macromolecules by NMR

2017 Chemistry Nobel : **Jacques Dubochet, Joachim Frank, and Richard Henderson** for structure determination of biomolecules with cryo EM

SMARTER crystallography approach

*****S**tructure determination by co**M**bining m**A**gnetic **R**esonance, compu**T**ation mod**E**ling and diff**R**actions*

High-flux sources
Rietveld (Bragg)
PDF (diffuse)

Powder Diffraction

⇒ **Average structural model**

HR (S)TEM
(Sub)Atomic resolution
EELS
Precession e diffraction

TEM

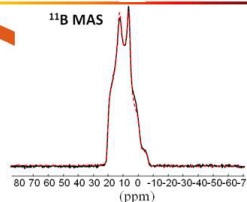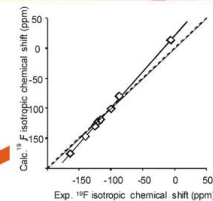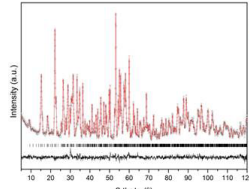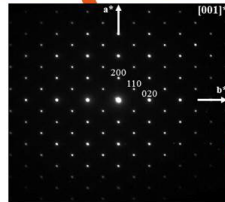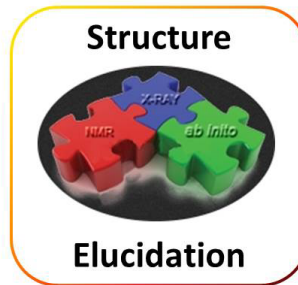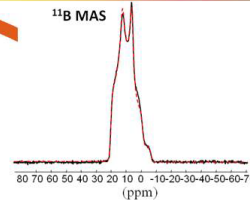⇒ **Symmetry / Nanometer scale**

SMARTER Crystallography

Structure

Elucidation

Structure determination by co**M**bining m**A**gnetic **R**esonance, compu**T**ation mod**E**ling and diff**R**actions

NMR Spectroscopy

^{11}B MAS

⇒ **Local state information**

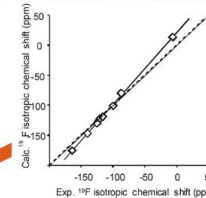**DFT calculations**

⇒ **Structure optimization/validation**

Very high magnetic fields
28.2 T commercial !
Very fast sample spinning
*120 kHz : **7 000 000 rd/min***

A variety of correlation methods
Multinuclear, 2D, 3D, etc...

Ab initio computations
Structure prediction
DFT GIPAW & PAW → NMR

Looking at it in different ways to better understand it

*taking benefits of constant technological
& methodological progresses*

Setting up the NMR group in Orléans with J.P Coutures and D. Massiot (1988-1992)

Francis Taulelle
(† 2021)

Outline

- **Complex superstructure of $M^{4+}P_2O_7$ materials** (thermal expansion prop.)

- **Melilite $La_2Ga_3O_{7.5}$ with interstitial O atoms** (oxide ion conductor)

- **Scheelite $Bi(Sr)VO_4$ with O defect** (oxide ion conductor)

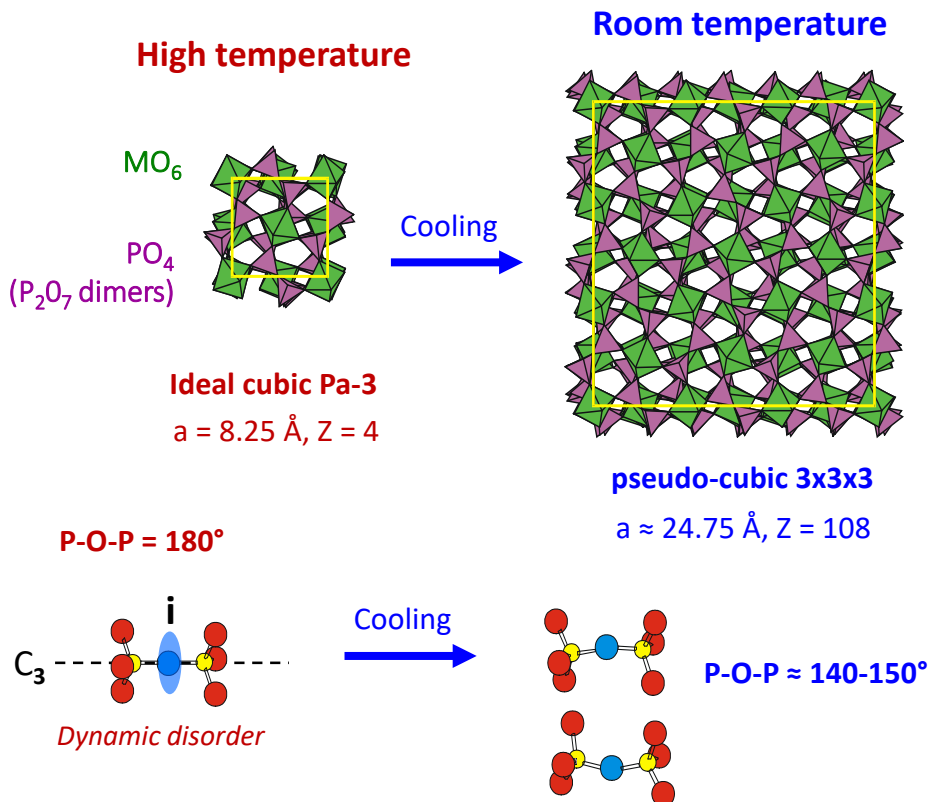- **Novel transparent polycrystalline ceramics** (optical)
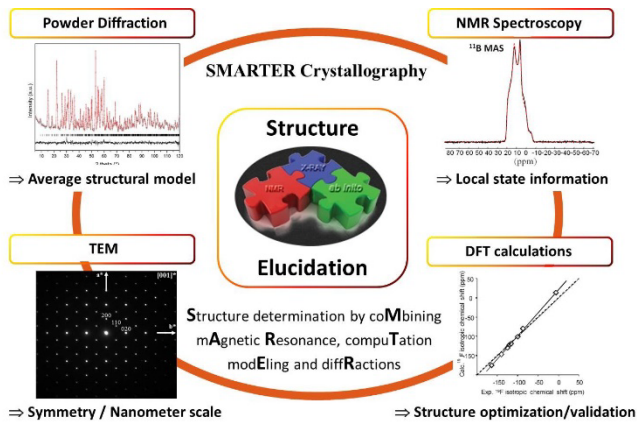
$M^{4+}P_2O_7$ compounds

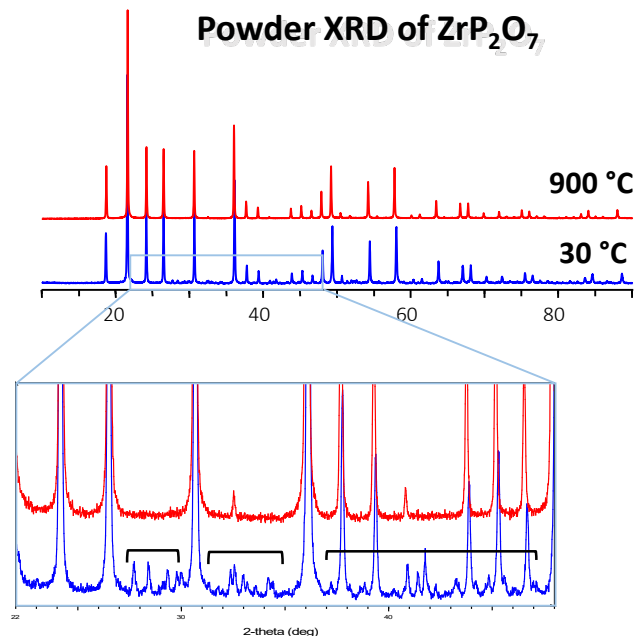$M^{4+}P_2O_7$ M = **Si, Ge, Ti, Zr, Hf**, Mo, W, **Sn**, Pb, …

J. Evans

- $M^{4+}A^{5+}_2O_7$ family (A = **P**, V or As)
- Simple cubic structure at high temperature (Pa-3, a ≈ 8Å) → **Weak, zero or negative thermal expansion**
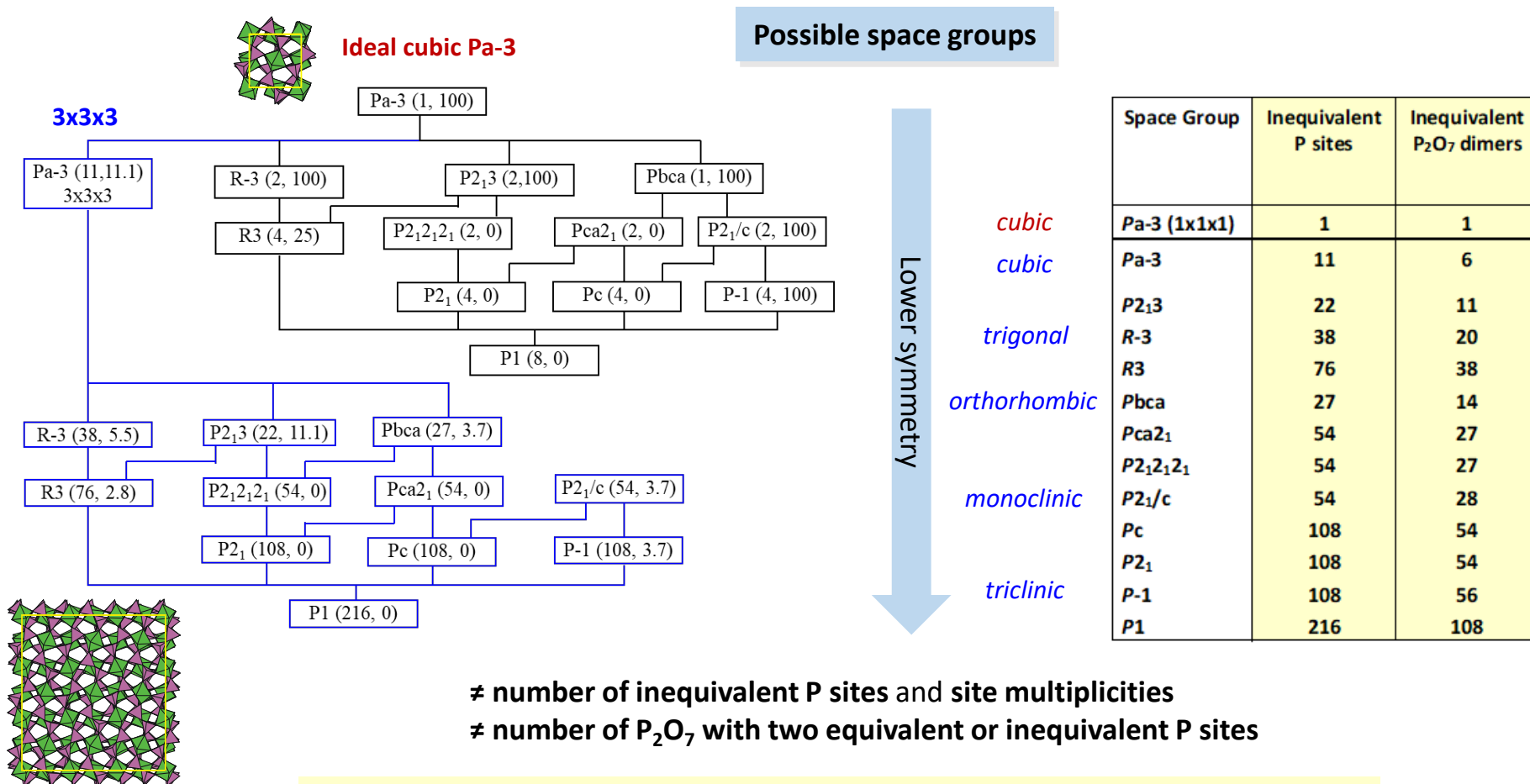- 3×3×3 superstructure at room temperature

Durham University

High temperature

Room temperature

MO_6

PO_4
(P_2O_7 dimers)

Cooling

Ideal cubic Pa-3

a = 8.25 Å, Z = 4

pseudo-cubic 3x3x3

a ≈ 24.75 Å, Z = 108

P-O-P = 180°

i

C_3

Dynamic disorder

Cooling

P-O-P ≈ 140-150°

Powder XRD of ZrP_2O_7

900 °C

30 °C

20   40   60   80

22   30   40
2-theta (deg)

Superstructure reflexion of weak intensities
→ Space group assignment difficult from powder XRD

Room temperature structures of $M^{4+}P_2O_7$ compounds

- **SiP_2O_7 and TiP_2O_7 : 3X3X3 cubic with Pa-3 @ room temp.**

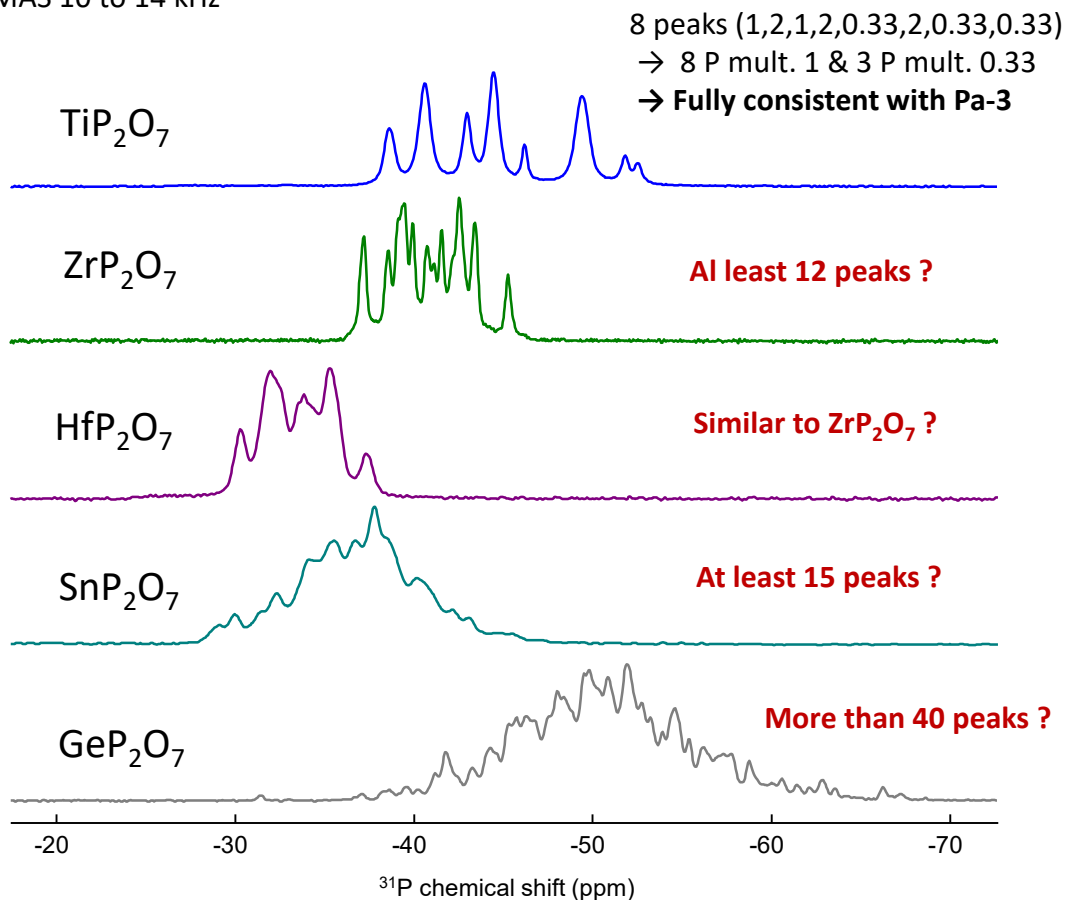- **ZrP_2O_7, HfP_2O_7 & SnP_2O_7 → Pa-3 ? Other SG ?**

Ideal cubic Pa-3

Possible space groups

3x3x3

Pa-3 (1, 100)

Pa-3 (11,11.1) 3x3x3

R-3 (2, 100)   P2$_1$3 (2,100)   Pbca (1, 100)

R3 (4, 25)   P2$_1$2$_1$2$_1$ (2, 0)   Pca2$_1$ (2, 0)   P2$_1$/c (2, 100)

P2$_1$ (4, 0)   Pc (4, 0)   P-1 (4, 100)

P1 (8, 0)

R-3 (38, 5.5)   P2$_1$3 (22, 11.1)   Pbca (27, 3.7)

R3 (76, 2.8)   P2$_1$2$_1$2$_1$ (54, 0)   Pca2$_1$ (54, 0)   P2$_1$/c (54, 3.7)

P2$_1$ (108, 0)   Pc (108, 0)   P-1 (108, 3.7)

P1 (216, 0)

Lower symmetry

Space Group	Inequivalent P sites	Inequivalent P_2O_7 dimers
Pa-3 (1x1x1)	1	1
Pa-3	11	6
P2$_1$3	22	11
R-3	38	20
R3	76	38
Pbca	27	14
Pca2$_1$	54	27
P2$_1$2$_1$2$_1$	54	27
P2$_1$/c	54	28
Pc	108	54
P2$_1$	108	54
P-1	108	56
P1	216	108

cubic — Pa-3 (1x1x1), Pa-3
cubic — P2$_1$3
trigonal — R-3, R3
orthorhombic — Pbca, Pca2$_1$, P2$_1$2$_1$2$_1$
monoclinic — P2$_1$/c, Pc, P2$_1$
triclinic — P-1, P1

≠ number of inequivalent P sites and site multiplicities
≠ number of P_2O_7 with two equivalent or inequivalent P sites

SMARTER approach → use ^{31}P solid-state NMR to probe local structure

^{31}P Magic Angle Spinning NMR of $M^{4+}P_2O_7$ compounds

$M^{4+}P_2O_7$ M = **Si, Ge, Ti, Zr, Hf**, Mo, W, **Sn**, Pb, …

^{31}P MAS NMR (spin ½, 100%)

B_0 = 7.0 T,
MAS 10 to 14 kHz

8 peaks (1,2,1,2,0.33,2,0.33,0.33)
→ 8 P mult. 1 & 3 P mult. 0.33
→ **Fully consistent with Pa-3**

Possible space groups

Space Group	Inequivalent P sites	Inequivalent P_2O_7 dimers
Pa-3 (1x1x1)	1	1
Pa-3	11	6
$P2_13$	22	11
R-3	38	20
R3	76	38
Pbca	27	14
$Pca2_1$	54	27
$P2_12_12_1$	54	27
$P2_1/c$	54	28
Pc	108	54
$P2_1$	108	54
P-1	108	56
P1	216	108

TiP_2O_7

ZrP_2O_7 **Al least 12 peaks ?**

HfP_2O_7 **Similar to ZrP_2O_7 ?**

SnP_2O_7 **At least 15 peaks ?**

GeP_2O_7 **More than 40 peaks ?**

-20   -30   -40   -50   -60   -70

^{31}P chemical shift (ppm)

^{31}P Magic Angle Spinning NMR of $M^{4+}P_2O_7$ compounds

$M^{4+}P_2O_7$ M = **Si, Ge, Ti, Zr, Hf**, Mo, W, **Sn**, Pb, ...

Presence of impurities, polymorphism ??

Check that all P sites (i.e. all ^{31}P NMR peak) belong to the same phase with **2D NMR !**

- Probing long-range spatial proximities between the P sites
- Recoupling of ^{31}P-^{31}P homonuclear dipolar interactions
- Longitudinal mixing (flip-flop) : RFDR

All P sites belong
to the same phase

Pa-3

ZrP$_2$O$_7$ SnP$_2$O$_7$

I.J. King, et al. *Chem. Commun.* 2001, 1766.
F. Fayon, et al. *C. R. Chimie* 2004, 7, 351.
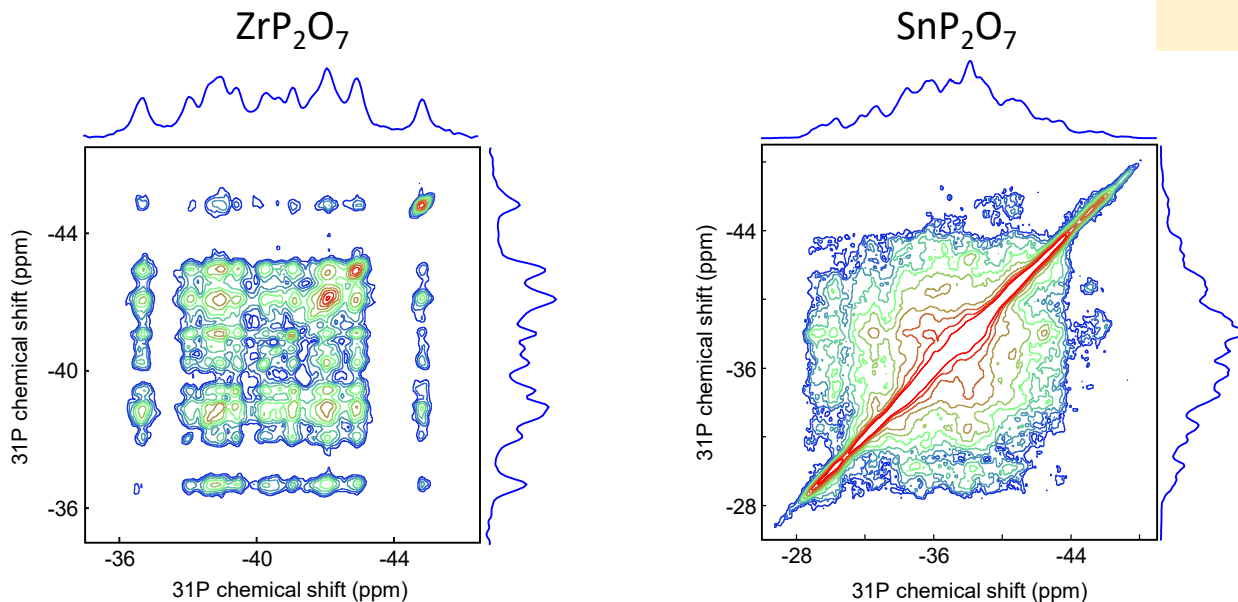
Probing P-O-P connectivity and the number of P_2O_7

^{31}P (spin ½, 100%) → Use **through-bond** ($^2J_{P-O-P}$) **or through-space** (dipolar short range) **to probe P-O-P connectivities**

→ **2D $^{31}P-^{31}P$ correlation (connectivity) spectra**

Improved resolution !! of distinct P sites and P_2O_7 dimers

Possible space groups

ZrP2O7

SnP2O7

Space Group	Inequivalent P sites	Inequivalent P_2O_7 dimers
Pa-3 (1x1x1)	1	1
Pa-3	11	6
$P2_13$	22	11
R-3	38	20
R3	76	38
Pbca	27	14
$Pca2_1$	54	27
$P2_12_12_1$	54	27
$P2_1/c$	54	28
Pc	108	54
$P2_1$	108	54
P-1	108	56
P1	216	108
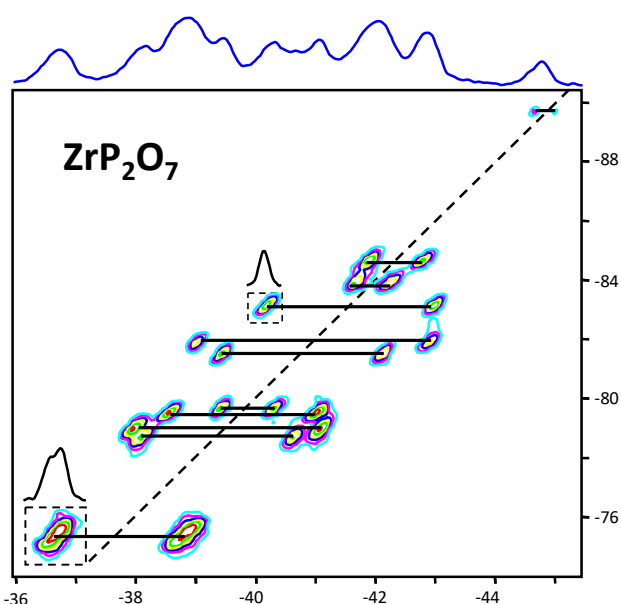
✧ 11 pairs of cross-peaks (one x3 intentity)
✧ 13 P_2O_7 dimers with two ineq. P sites
✧ 1 P_2O_7 with two equivalent P sites (inversion center)

→ orthorhombic with Pbca
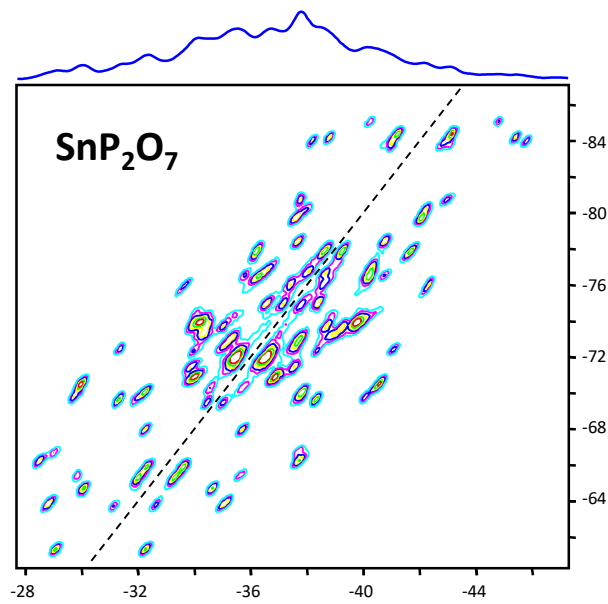
✧ 49 pairs of cross-peaks (1 x3 and 3 x2 intensities)
✧ At least 98 distinct P sites (likely **108**)

→ monoclinic with $P2_1$ or Pc space group

I.J. King, et al. *Chem. Commun.* 2001, 1766.

F. Fayon, et al. *Chem. Mater.* **15**, 2234-2239 (2003).

Room temperature structures of $M^{4+}P_2O_7$ compounds

$M^{4+}P_2O_7$ M = **Si, Ge, Ti, Zr, Hf**, Mo, W, **Sn**, Pb, …

Rietveld refinement of PXRD (synchrotron) **and/or NPD data**

ZrP_2O_7 & HfP_2O_7 (Pbca, 136 atoms)

^{31}P NMR toolbox

ZrP_2O_7, HfP_2O_7 ⟶ *Orthorhombic Pbca*

SnP_2O_7, GeP_2O_7 ⟶ *Monoclinic Pc or $P2_1$*

Cubic Pa-3

Orthorhombic Pbca
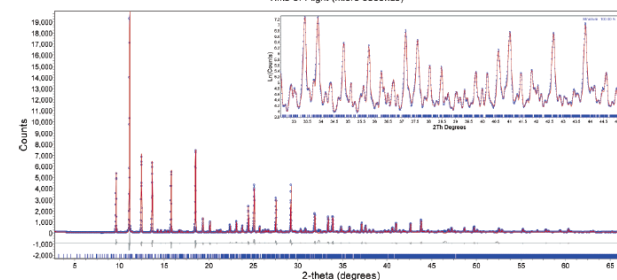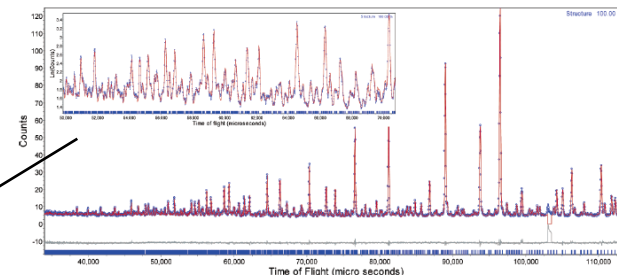
G. Stinton et al, *Inorg. Chem.* 45 4357 **2005**
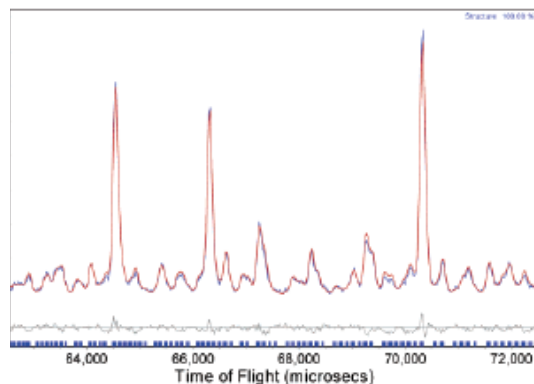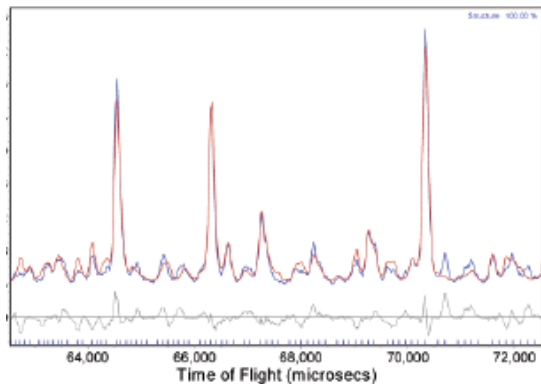
Melilite compounds with extra oxide ions

Melilite $A_2B(M_2O_7)$

Tetragonal ($P\text{-}42_1$) a $\sim$8 Å, c $\sim$5 Å

layers of coner-sharing MO_4 tetrahedra
layers of A,B cations → **Ionic conduction properties**
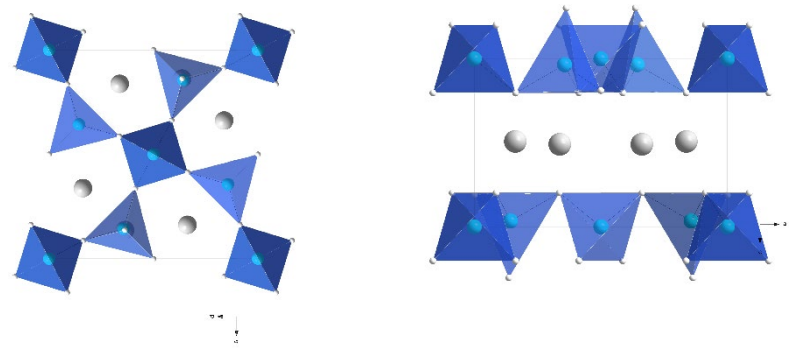
Interstitial oxide ion conductivity in the
layered tetrahedral network melilite
structure

XIAOJUN KUANG[1], MARK A. GREEN[2,3], HONGJUN NIU[1], PAWEL ZAJDEL[2,4], CALUM DICKINSON[1],
JOHN B. CLARIDGE[1], LAURENT JANTSKY[1] AND MATTHEW J. ROSSEINSKY[1]*

Nature Materials, 2008

$LaSrGa_3O_7$ → $La_{1+x}Sr_{1-x}Ga_3O_{7+x/2}$ ($0 \leq x \leq 0.64$)
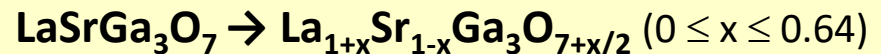
Extra oxygen sites → Oxide ion conduction
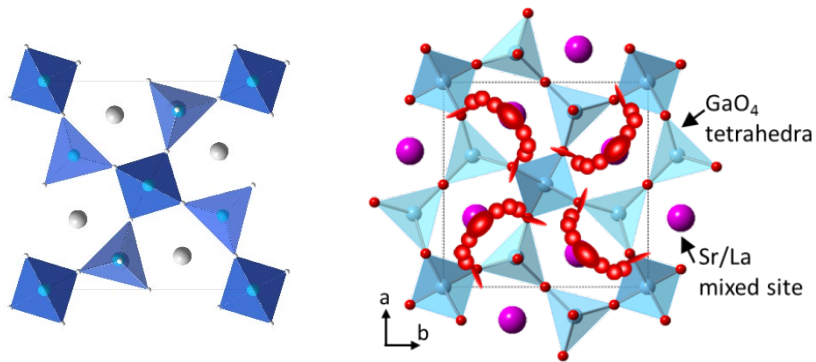
(x=0.54): 0.1 S.cm-1 @ 800°C   (fuel cell applications)

Melilite compounds with extra oxide ions : $La_2Ga_3O_{7.5}$

M. Allix   M. Pitcher

CHEMISTRY OF MATERIALS
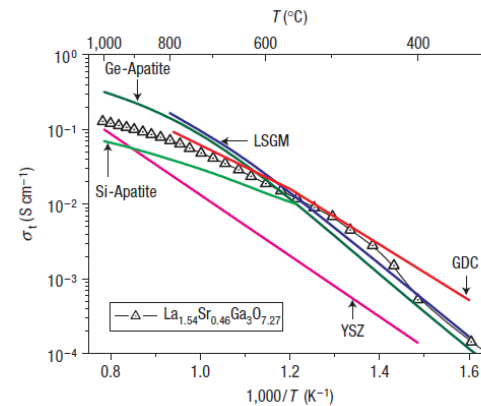
pubs.acs.org/cm   Article

$La_2Ga_3O_{7.5}$: A Metastable Ternary Melilite with a Super-Excess of Interstitial Oxide Ions Synthesized by Direct Crystallization of the Melt

Jintai Fan, Vincent Sarou-Kanian, Xiaoyan Yang, Maria Diaz-Lopez, Franck Fayon, Xiaojun Kuang, Michael J. Pitcher,* and Mathieu Allix*

Undercooled Melt
1800°C

Solid-state
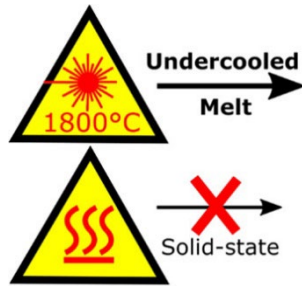
Synthesis of **$La_2Ga_3O_{7.5}$ (x = 1, full substitution!)**
by **direct crystallization from an undercooled melt**
(aerodynamic levitation under O_2 atm., precursors: La_2O_3 & Ga_2O_3)

CO_2 Laser
Sample
Nozzle
Carrier Gas
5 mm
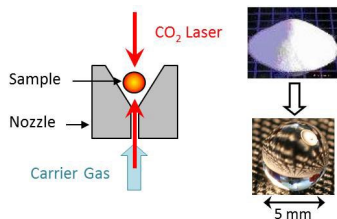
$La_2Ga_3O_{7.5}$ is stable up to 830 °C

Full occupancy of the interstitial O site

→ *Reduced oxide conductivity* ☹

→ *Structural model* ☺

J. Fan et al., Chem Mater, 2020
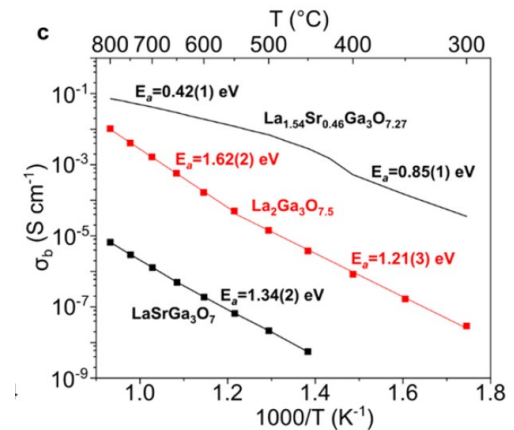
Melilite compounds with extra oxide ions : $La_2Ga_3O_{7.5}$

Laboratory powder XRD of $La_2Ga_3O_{7.5}$

PDF 04-017-7922 Ca0.36La1.64Ga3O7.32 Calcium Gallium Lanthanum Oxide
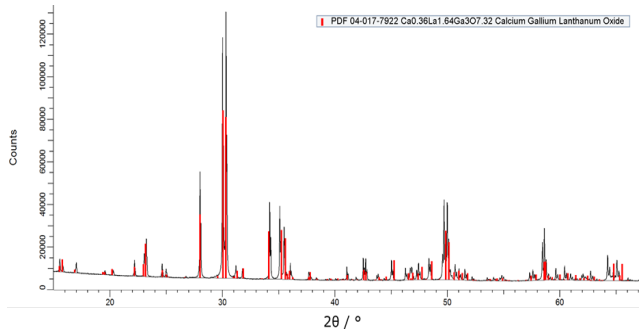
Similar to the **pseudo-orthorhombic melilite $La_{1.64}Ca_{0.36}Ga_3O_{7.32}$** (PDF 04-017-7922)
Li et al., *Angew. Chemie Int. Ed.* **2010**

→ **Provisional structural model with *P*1**

Combined Rietveld refinement with P1

- *Description of melilite **framework & oxide interstitial sites***
- *No symmetry constraints on the possible interstitial **oxide ion orderings***
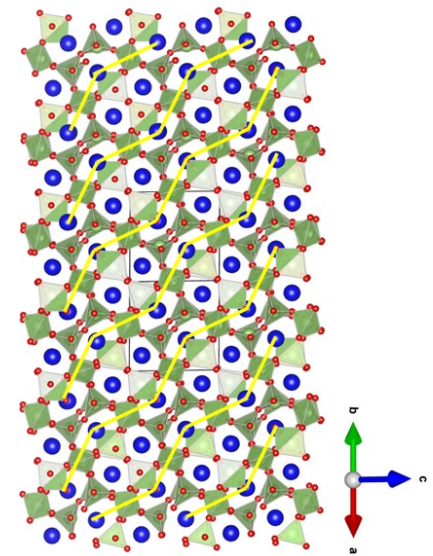
Synchrotron XRD of $La_2Ga_3O_{7.5}$

11-BM, APS, Argonne, USA
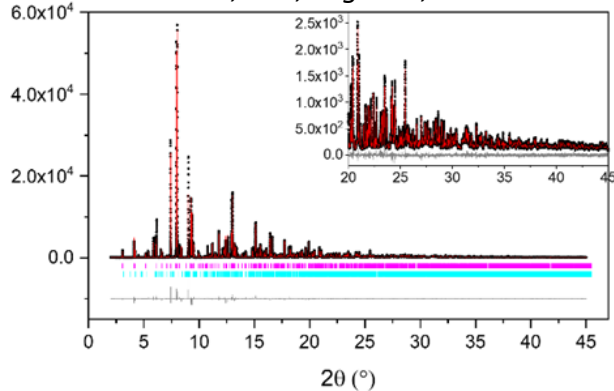
Neutron diffraction of $La_2Ga_3O_{7.5}$

D2B, ILL, Grenoble, Fr
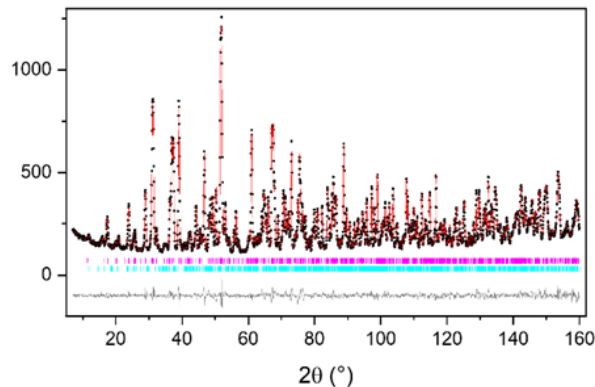
Pseudo-ortho. (P1)
a = 9.6032, *b* = 9.5999, *c* = 9.6004 Å,
α = 106.59, β = 108.13, γ = 113.81°

52 At. Pos. : **8 La, 12 Ga, 32 O**

→ **Chain-ordering of O_{int}**

Melilite compounds with extra oxide ions : $La_2Ga_3O_{7.5}$

Provisional *P*1
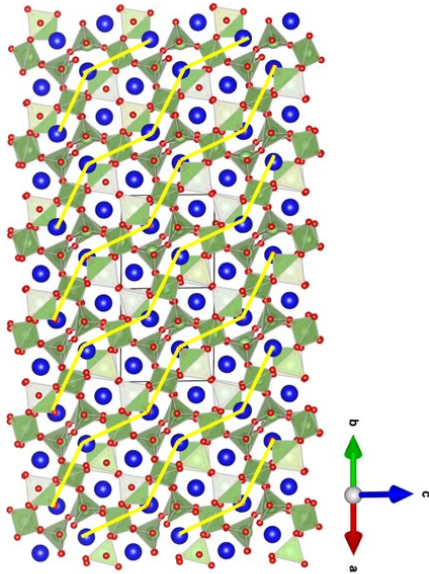
Pseudo orthorhombic
a = 9.6032, b = 9.5999, c = 9.6004 Å,
α = 106.59, β = 108.13, γ = 113.81°

P1 : 8 La, 12 Ga, 32 O

SMARTER approach....

DFT modelization

optimization of all atomic positions
(cell parameters fixed to exp. values)

Symmetry search

GaO_4 → GaO_4+O_{int} = GaO_5

Final *Ima2*
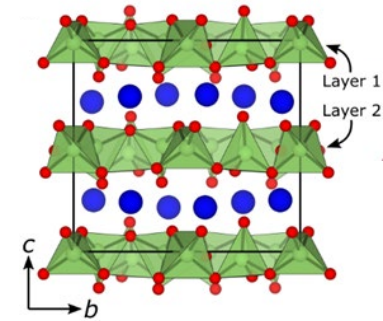
Orthorhombic
√2a x √2a x 2c expansion of the parent cell
Ima2 space group
3 La, 5 Ga, 10 O sites

Layer 1 (z = 0)   Layer 2 (z = 1/2)
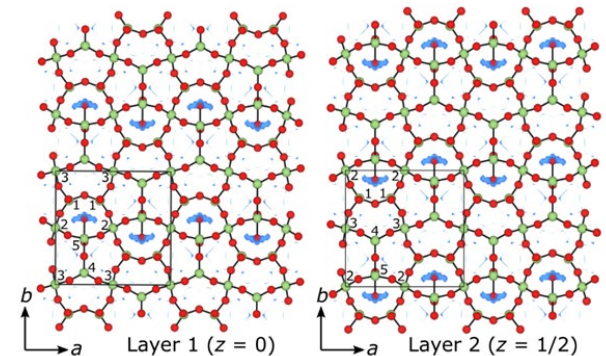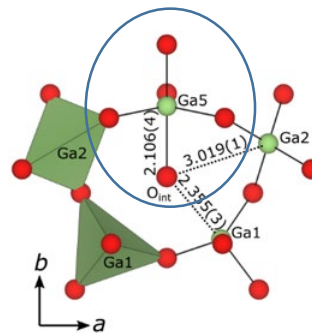
Full long-range ordering of O_{int}
within the [$Ga_3O_{7.5}$] layers

Five Ga sites, formation of GaO_5 ? → *Solid-state ^{71}Ga NMR*

Probing the Ga environment with ^{71}Ga NMR

SMARTER approach….

^{71}Ga NMR
 I = 3/2 , strong quadrupolar interactions (broadening)

Very-high magnetic fields
Very fast magic angle spinning *(0.7mm probe, up to 110 kHz)*

^{71}Ga NMR @ 20T, MAS 100 kHz

^{71}Ga STMAS @ 100 kHz
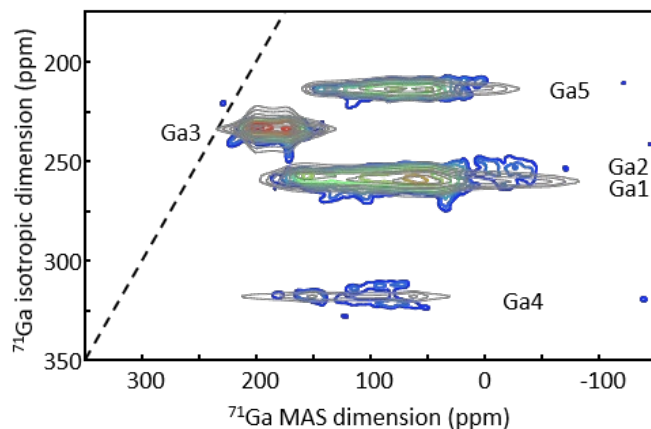
^{71}Ga MAS quantitative @ 100 kHz

5 inequivalent Ga sites
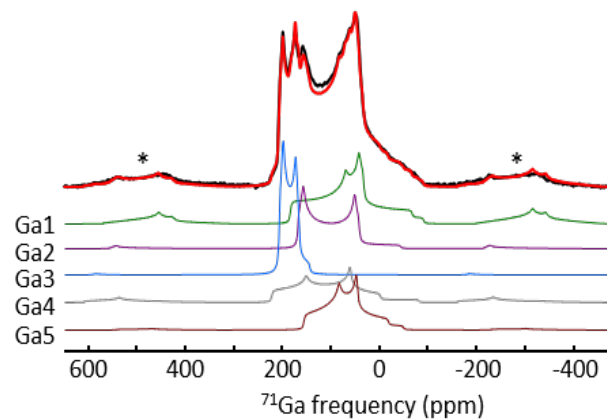
with 2:1:1:1:1 multiplicities

→ consistent with **Ima2** space group

Melilite compounds with extra oxide ions : $La_2Ga_3O_{7.5}$

SMARTER approach….

DFT GIPAW computation of ^{71}Ga NMR using the refined Ima2 model

Combined XRD and NPD refinement with Ima2 structural model

Synchrotron XRD of $La_2Ga_3O_{7.5}$
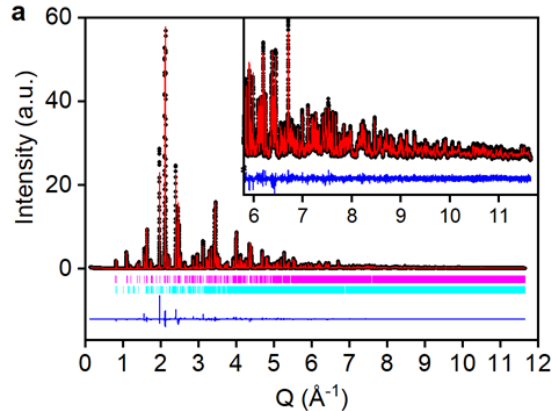
Neutron diffraction of $La_2Ga_3O_{7.5}$
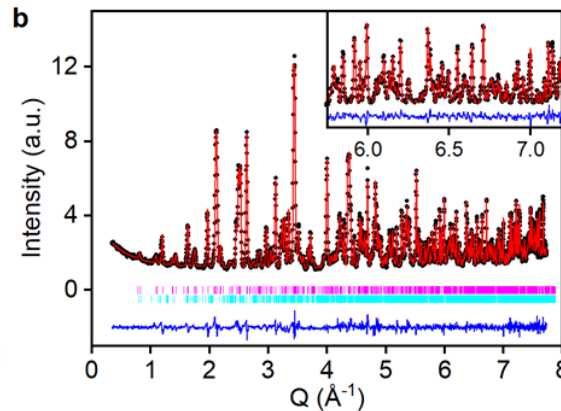
Experimental ^{71}Ga STMAS
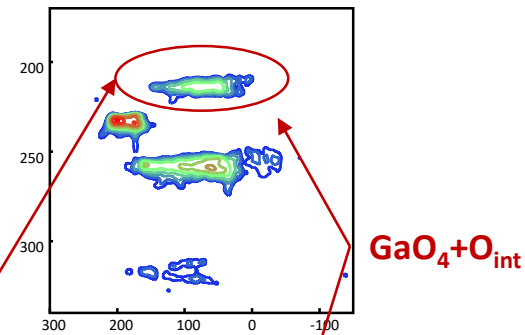
GaO_4+O_{int}

Theoretical GIPAW ^{71}Ga STMAS
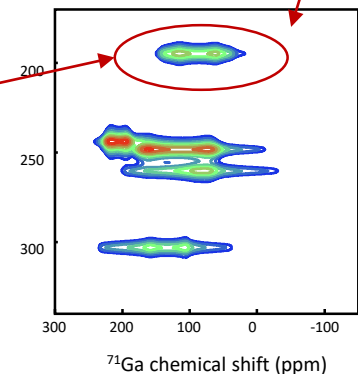
5 Ga, 3 La, 10 O in the asymmetric unit

a = 11.4701 b = 11.2674 c = 10.4804 Å,

R_{wp} = 7.49 %, χ^2 = 3.06 (χ^2 = 2.98 for $P1$)

Structural model accounting for both long-range ordering and local structure
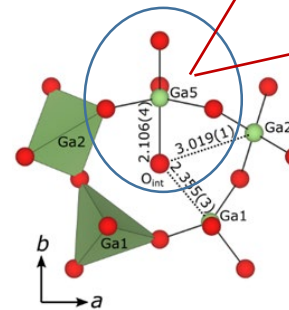
$BiVO_4$ and $Bi_{1-x}Sr_xVO_{4-x/2}$ Scheelite compounds

Scheelite materials for oxide ion conductivity applications

- **$BiVO_4$ Scheelite structure**
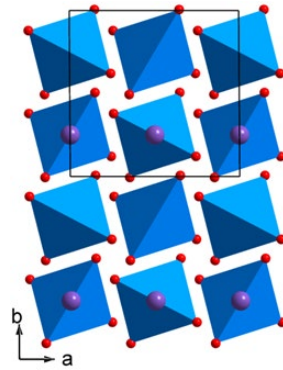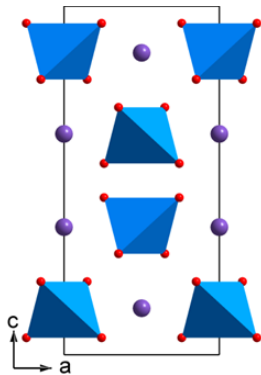
- Isolated VO_4 tetrahedral
- AO_8 polyhedra

- Monoclinic (I2/b)
- Tetragonal (I4$_1$/a) @ 250 °C

- **Bi^{3+} for Sr^{2+} substitution** → **Oxide ion vacancies in the tetrahedral network**

  → *Improved oxide anionic conductivity*
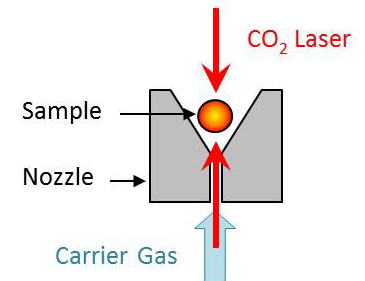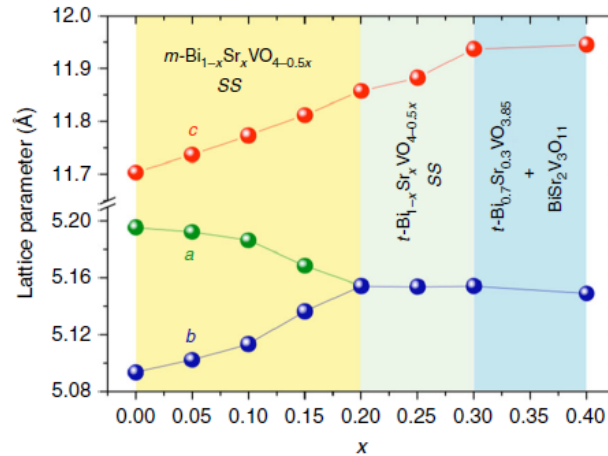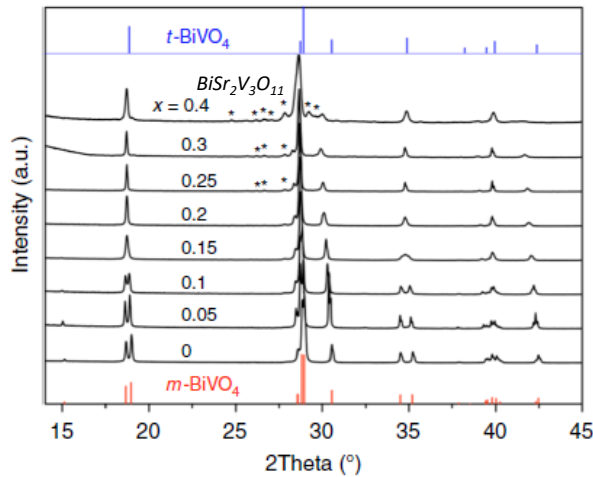

M. Allix   A. Fernández Carrión   X. Kuang

Investigation of the $Bi_{1-x}Sr_xVO_{4-x/2}$ compounds

BiVO$_4$ and Bi$_{1-x}$Sr$_x$VO$_{4-x/2}$ Scheelite compounds

Synthesis by direct crystallization from the melt - Aerodynamic levitation

Extended solid-solution range of Bi$_{1-x}$Sr$_x$VO$_{4-x/2}$ up to x ~ 0.3
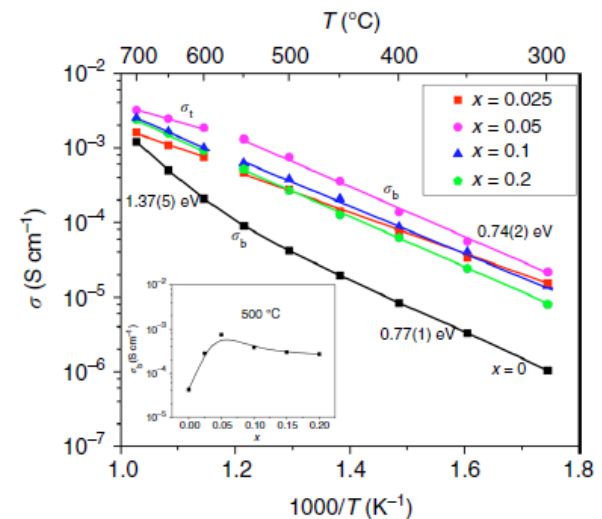
A. Fernández Carrión

Monoclinic → tetragonal scheelite with increasing x (Sr content)

Improved oxide anionic conductivity (x10) vs BiVO$_4$
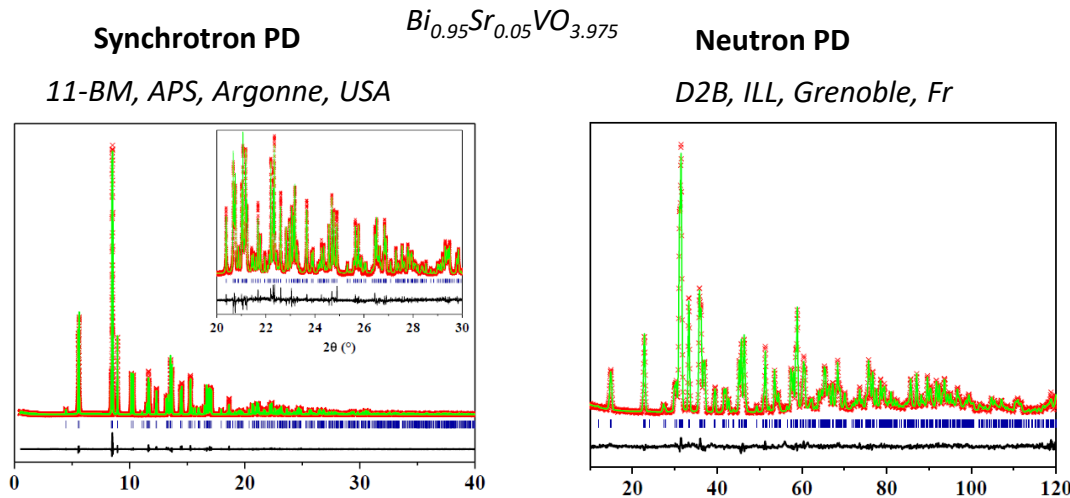**Optimal for Bi$_{0.95}$Sr$_{0.05}$VO$_{3.975}$**
(σ ~ 5.10^{-2} S/cm @ 700°C)

$BiVO_4$ and $Bi_{1-x}Sr_xVO_{4-x/2}$ Scheelite compounds

Mechanism for accommodation of O vacancies in the network of tetrahedral ?

Formation of VO_3 units or pairing of VO_4 units to form V_2O_7 dimers ? (like Ga_2O_7 units in $La_{1-x}Ba_{1+x}GaO_{4-x/2}$)

$Bi_{0.95}Sr_{0.05}VO_{3.975}$

Synchrotron PD

11-BM, APS, Argonne, USA

Neutron PD

D2B, ILL, Grenoble, Fr

- **Monoclinic scheelite I2/m**
- **$Bi_{0.893(2)}Sr_{0.107(2)}VO_{3.918(6)}$** **composition**
- Bi/Sr mixed site $(Bi_{0.9}Sr_{0.1})$ **→ oxygen vacancies**
- **strong positional disorder** (O, Bi, Sr)
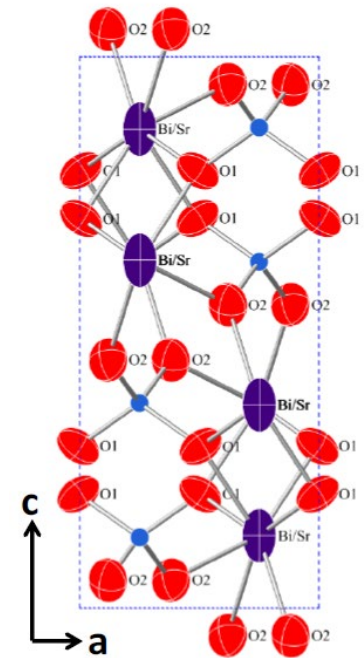
No observable residual scattering density in SPD & NPD Fourier difference maps !

Average structure – No evidence of O defects

BiVO$_4$ and Bi$_{1-x}$Sr$_x$VO$_{4-x/2}$ Scheelite compounds

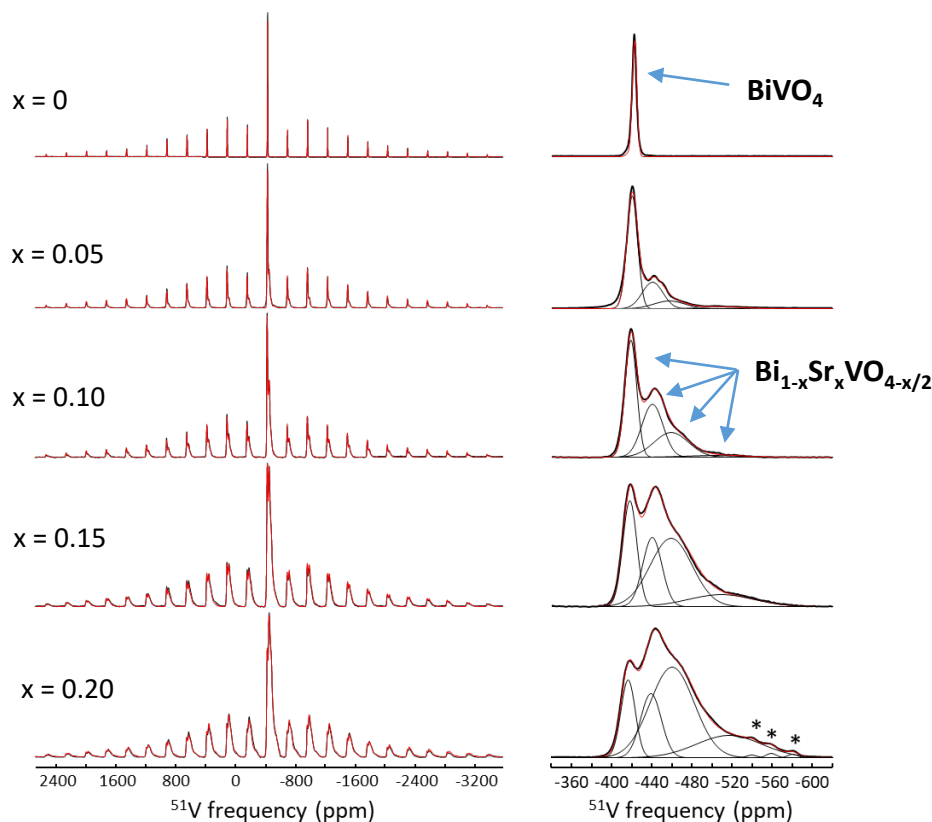**SMARTER approach....** *Probing the presence of V$_2$O$_7$ dimers with ^{51}V NMR*

^{51}V NMR
 I = 5/2 , moderate quadrupolar interaction, Chemical Shift Anisotropy

Very-high magnetic fields & Very fast magic angle spinning
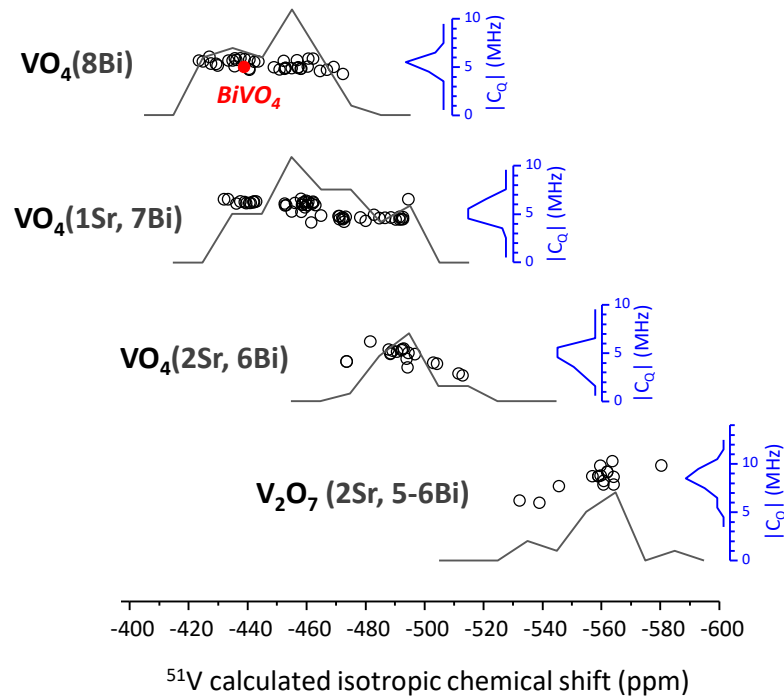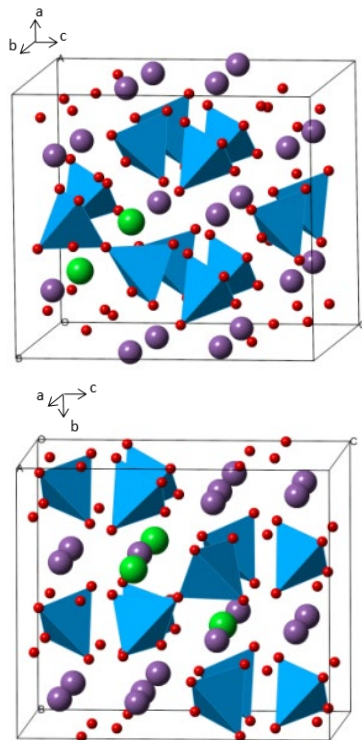
^{51}V NMR @ 20T, MAS 60 kHz

x = 0 → BiVO$_4$

x = 0.05

x = 0.10 → Bi$_{1-x}$Sr$_x$VO$_{4-x/2}$

x = 0.15

x = 0.20

2400 1600 800 0 -800 -1600 -2400 -3200
^{51}V frequency (ppm)

-360 -400 -440 -480 -520 -560 -600
^{51}V frequency (ppm)

- *Bi/Sr substitution induces a variety of ^{51}V resonances*

- *Second neighbors (Bi/Sr) of VO$_4$?*
- *V$_2$O$_7$?*

→ DFT GIPAW computation of ^{51}V NMR chemical shift

BiVO$_4$ and Bi$_{1-x}$Sr$_x$VO$_{4-x/2}$ Scheelite compounds

SMARTER approach…. *Probing the presence of V$_2$O$_7$ dimers with ^{51}V NMR*

- Build **2x2x1 supercell** models of **Sr$_{0.125}$Bi$_{0.975}$O$_{3.937}$**

→ Accommodation of **one O vacancy** and **two Sr** cations → formation of **one V$_2$O$_7$** defect (8 possibilities)

- DFT optimization of atomic positions → relaxed structures with realistic Sr-O distances
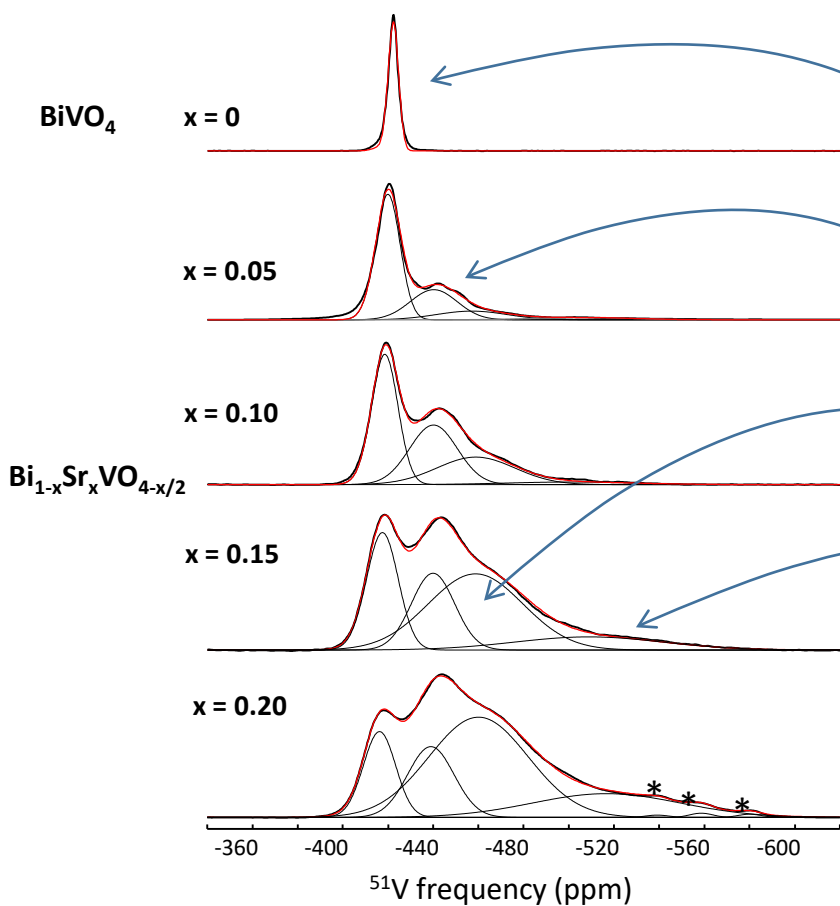- DFT GIPAW → ^{51}V NMR parameters

^{51}V NMR parameters (CS & Quad.) of possible local environnements

BiVO$_4$ and Bi$_{1-x}$Sr$_x$VO$_{4-x/2}$ Scheelite compounds

SMARTER approach.... *Probing the presence of V$_2$O$_7$ dimers with ^{51}V NMR*

^{51}V NMR @ 20T, MAS 60 kHz

DFT-GIPAW computations
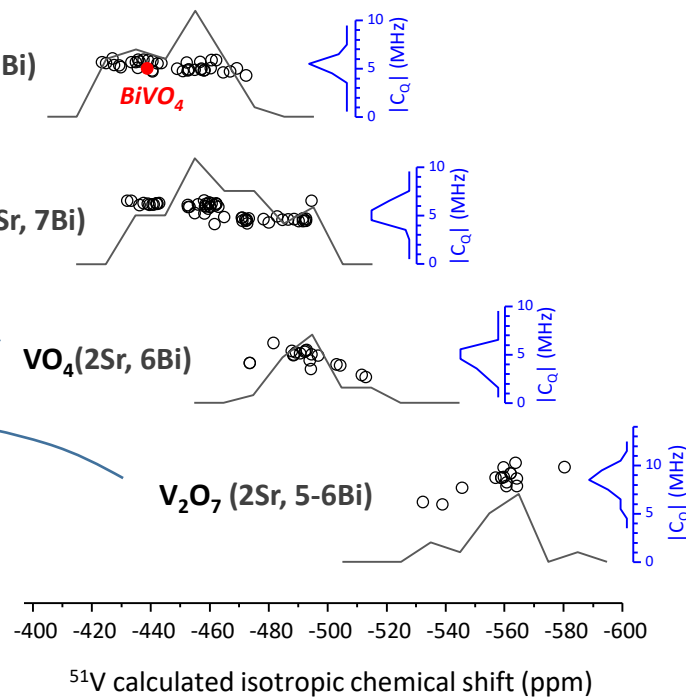
- **Unambiguous assignment of ^{51}V resonances**
- **Evidence for formation of V$_2$O$_7$ defects**

BiVO$_4$ and Bi$_{1-x}$Sr$_x$VO$_{4-x/2}$ Scheelite compounds
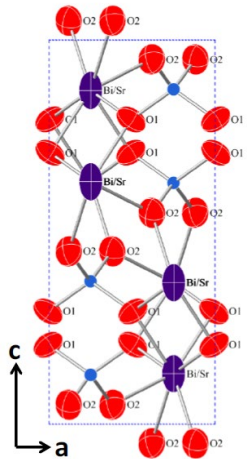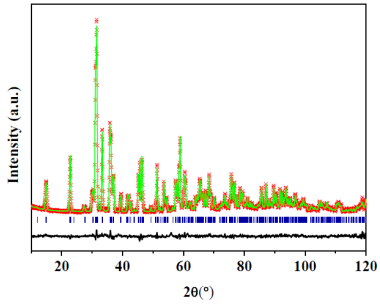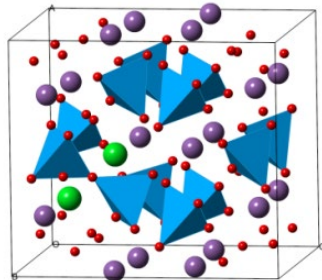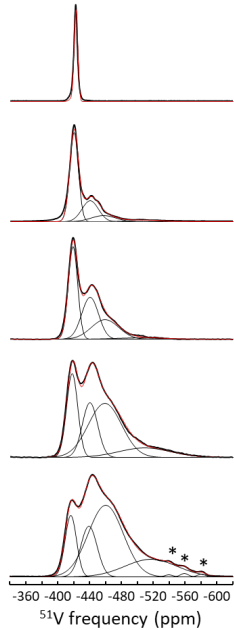
SPD & NPD

^{51}V NMR @ 20T

^{51}V frequency (ppm)

Average (long range) and local structure description
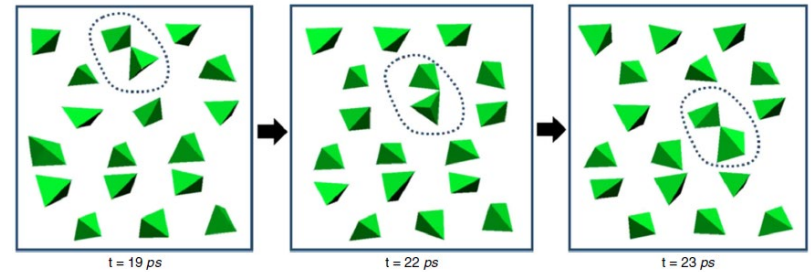
...SMARTER approach....

O vacancies migration mechanism
Molecular Dynamic simulations *(classical, DL-Poly)*

simulation box : **8 × 8 × 4** unit cells , **6112** atoms
Sr$_{0.0625}$Bi$_{0.9375}$VO$_{3.96875}$ composition
300 ps trajectory @ 1400K

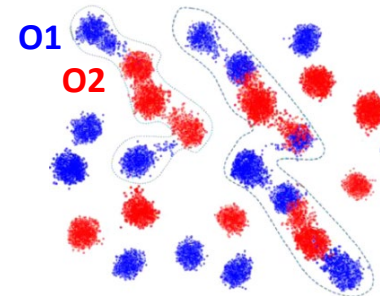**MD trajectory @ 1400 K**

t = 19 ps   t = 22 ps   t = 23 ps

long-range migration of O vacancies
→ continuous breaking and reforming of V$_2$O$_7$

Cooperative mechanism :
Rotation and deformation of neighboring VO$_4$
transfer O anions between V$_2$O$_7$ and VO$_4$

All oxygen atoms (O1, O2) are involved

O1
O2

...looking forward to O migration by ^{17}O NMR....
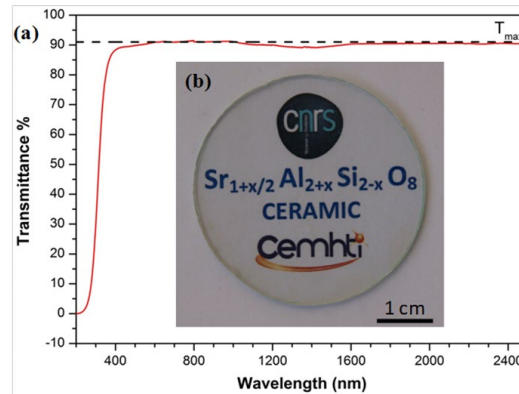
New transparent polycristalline ceramics

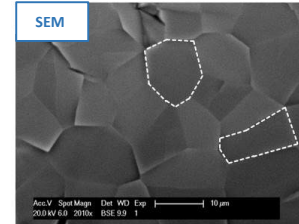**Novel transparent ceramics** obtained by **full congruent crystallization from glasses**

M. Allix   C. Genevois

(a) (b) $Sr_{1+x/2} Al_{2+x} Si_{2-x} O_8$ CERAMIC — Cemhti — 1 cm
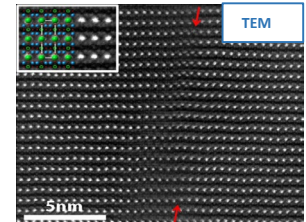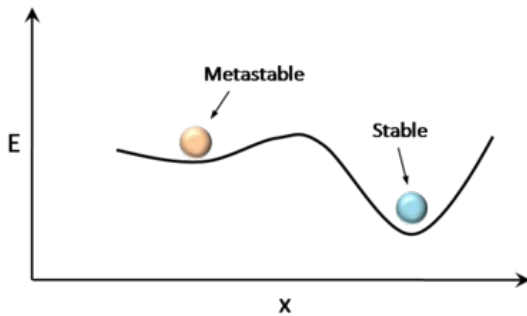
High transparency

No porosity
Mosaic microstructure

Very thin grain boundaries

Crystallization from glass
(out of equilibrium state)

Metastable / Stable

Metastable phases with **new** (unknown) **structures**   →   **SMARTER approach**
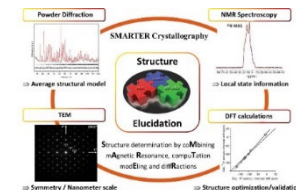
New transparent polycristalline ceramics : Aluminosilicate feldspar

SiO$_2$

SrAl$_2$Si$_2$O$_8$

SrO   SrAl$_2$O$_4$ Al$_2$O$_3$
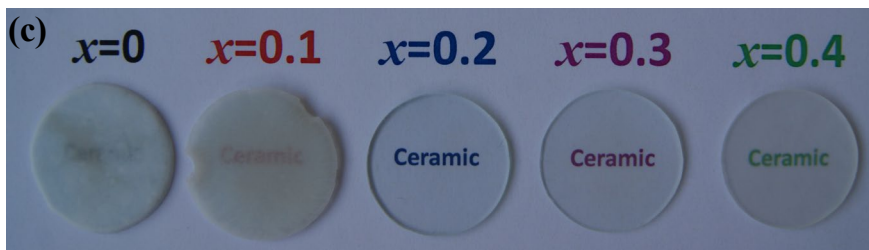mole fraction

Feldspar mineral family

Aluminium (gallium) tectosilicate minerals : $M^+AlSi_3O_8 - M^{2+}Al_2Si_2O_8$
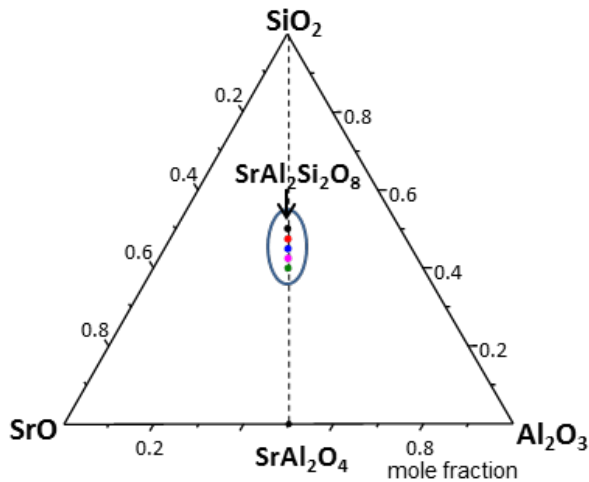
- **Good glass-forming ability**
- **Congruent crystallization**
- **Fully polymerized tetrahedral network**
  M^+/M^{2+} cations charge balance AlO_4^-, GaO_4^-

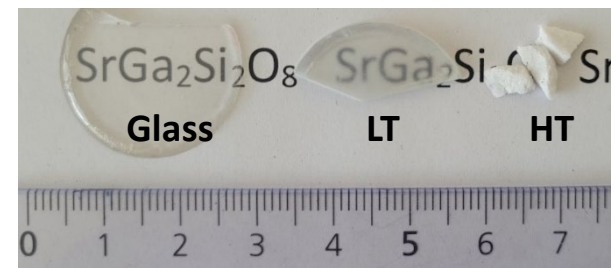- **Polymorphism**
  Feldspar, Paracelcian (3D) or Hexacelcian (2D)

M^{2+}
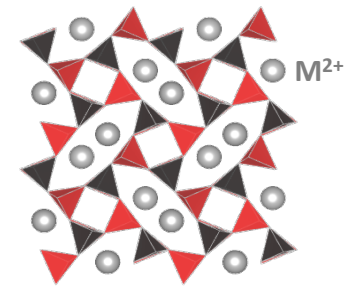
Sr$_{1+x/2}$Al$_{2+x}$Si$_{2-x}$O$_8$ ceramics ($0 \leq x \leq 0.4$)

(c) x=0   x=0.1   x=0.2   x=0.3   x=0.4

K. Al Saghir et al., *Chem. Mater.* 2015.

SrGa$_2$Si$_2$O$_8$ ceramics

SrGa$_2$Si$_2$O$_8$ SrGa$_2$Si   Sr
Glass   LT   HT

0   1   2   3   4   5   6   7

Annealing at   Annealing at
875°C / 18h   1200°C/1h

Variation of the transparency with composition → structural effect ?

Long range (average) structure

$Sr_{1+x/2}Al_{2+x}Si_{2-x}O_8$ solid-solution
$(0 \leq x \leq 0.4)$

SPD & NPD

STEM-HAADF

- **Pseudo-2D layered structure**
- **Hexagonal** with **P6$_3$/mcm**
(hexacelcian)

Mixed Al/Si

Sr2 (partial)

K. Al Saghir et al., *Chem. Mater.* 2015.

$SrGa_2Si_2O_8$

SPD & NPD

STEM-HAADF

- **3D network of tetrahedra**
- **Monoclinic** (quasi-orthorhombic) **P 21/a** (paracelcian)
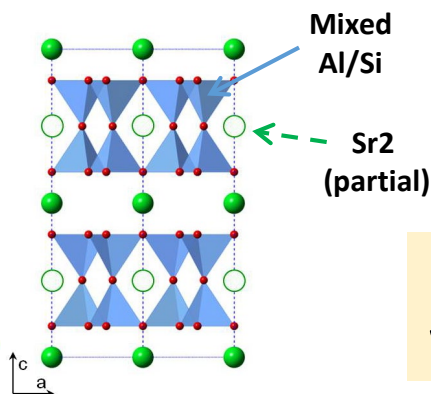
Mixed Al/Si
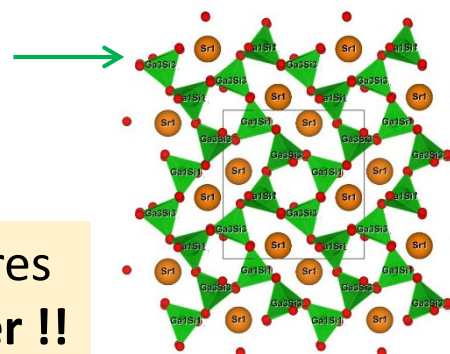
Different structures **with local disorder !!**

M. Allix   C. Genevois

Si/Al chemical disorder in ceramics : ^{29}Si and ^{27}Al NMR

Probing the Al/Si chemical disorder using ^{29}Si and ^{27}Al MAS NMR
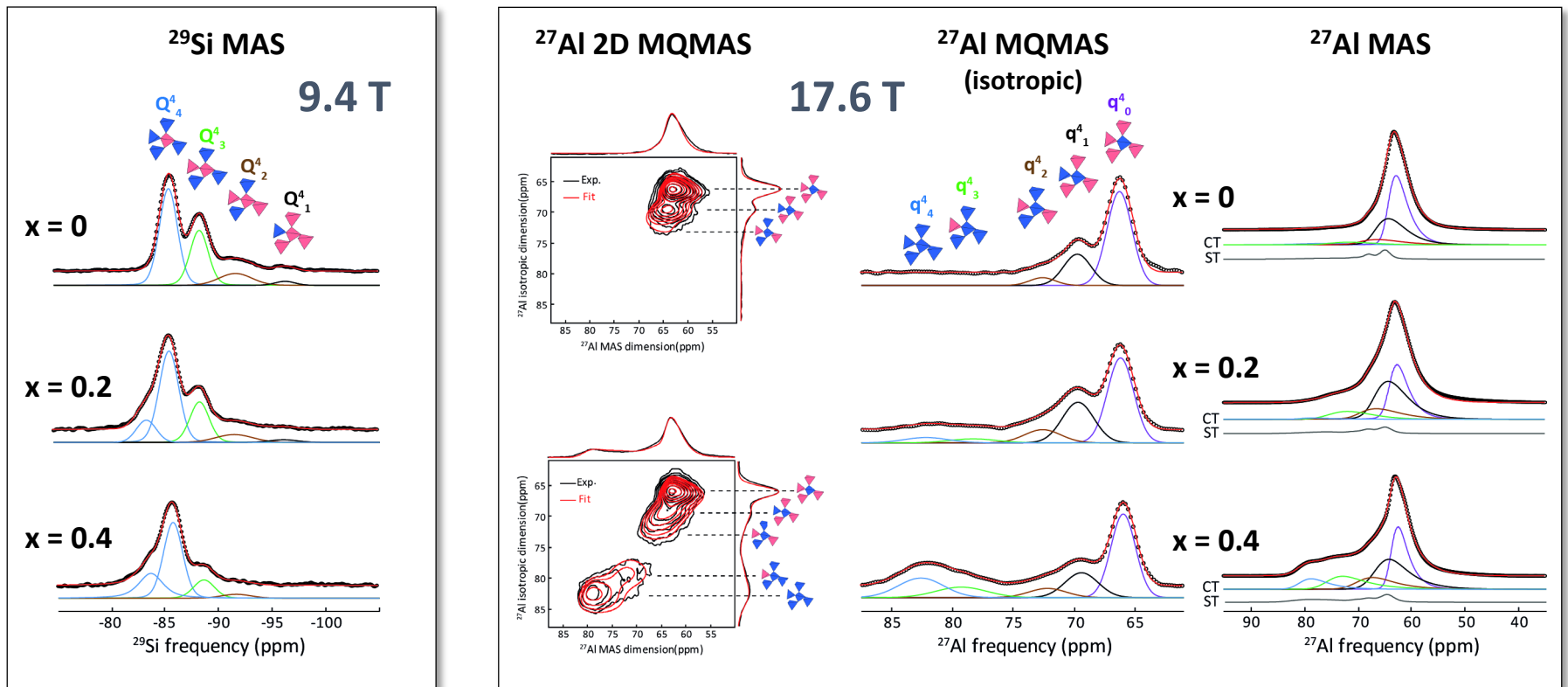
Identification and quantification of the various Si (Q^4_{mAl}) and Al (q^4_{mAl}) units in the structure

SPD → long-range average structure (HR-TEM)

^{29}Si / ^{27}Al NMR → local structure and degree of Si/Al local disorder

(departure from Lowenstein rule configurational entropy)

K. Al Saghir et al., *Chem. Mater.* 2015.

Building structural models from diffraction and NMR data

Supercell approximation of the substitutional disorder

« Supercell » program
Okhotnikov et al., J. Cheminform 2016.

- **2x2x1 supercell of the average unit cell** (104 atoms)

- **Generating all possible configurations** (Al/Si ordering)

- **Energy constraints** **(highest coulombic energy structures excluded)**
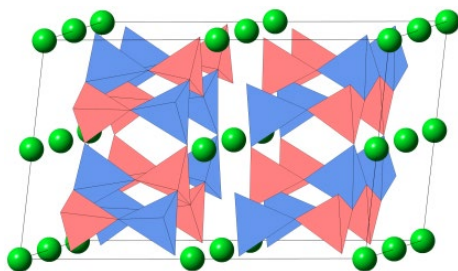
x = 0.25

Coulombic energy (eV)

-4200
-4210
-4220
-4230
-4240

Possible configurations   ~ 39 10⁶

Local charge compensation of the extra Sr atom (for x= 0.25)

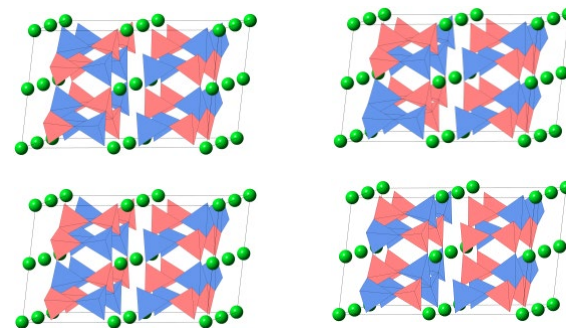- **Random selection with Q^n_{mAl} and q^n_{mAl} populations as constraints**

2x2x1 model

Set of structures
### (effective medium approximation)

- **DFT-PBE geometry optimization (atomic positions)**

only averaged bond lengths and angles available from diffraction

→ **Periodic DFT GIPAW computations (CASTEP) of NMR shielding and EFG tensors**

K. Al Saghir et al., *Chem. Mater.* 2015.

Ceramics : selected structural models

First-principle calculations (DFT-GIPAW) of NMR spectra from structural models
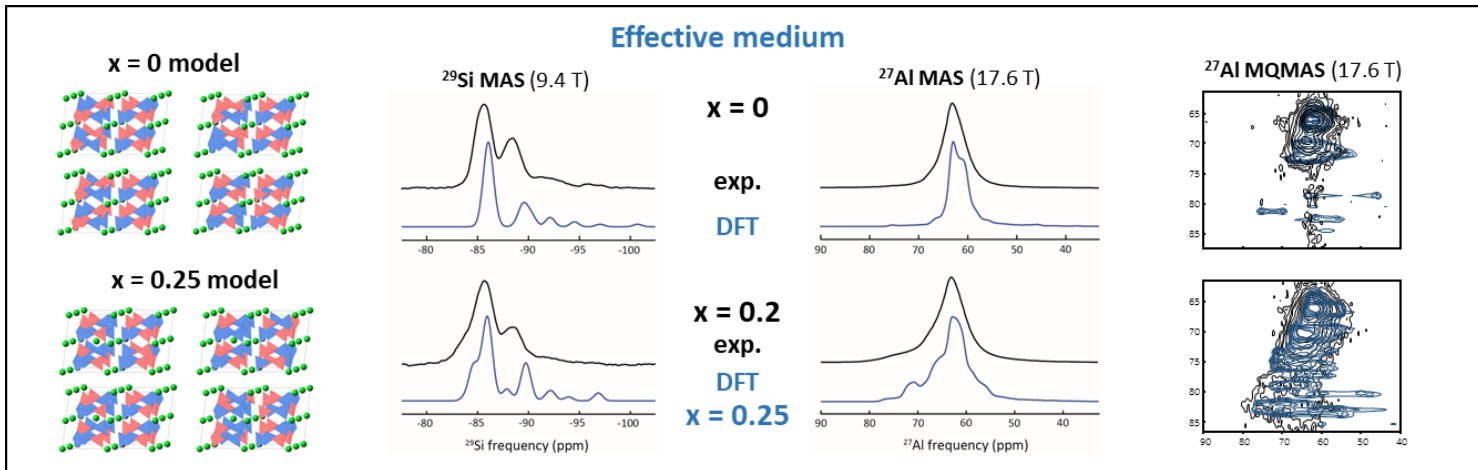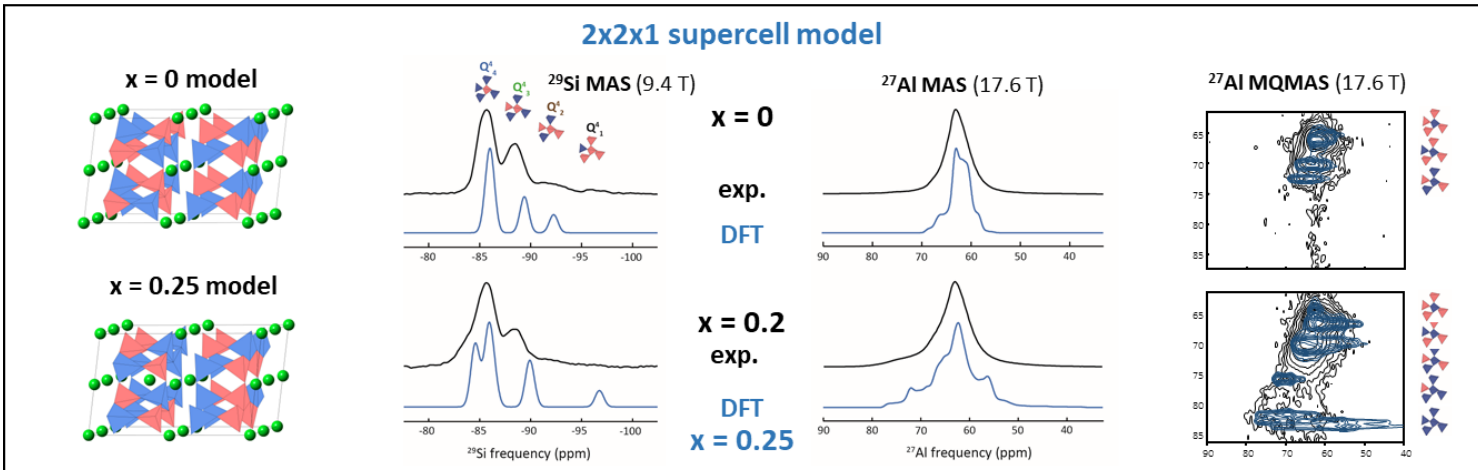
Models capture long-range structure & account partly for local structures

→ *computation of properties* (birefringence)

Ceramics : DFT computation of birefringence from models

• **Dielectric function**

$$\varepsilon(\omega) = \varepsilon_1(\omega) + i\,\varepsilon_2(\omega)$$

→ **refractive indexes**

$$n = \left(\frac{\sqrt{\varepsilon_1^2 + \varepsilon_2^2} + \varepsilon_1}{2}\right)^{1/2}$$

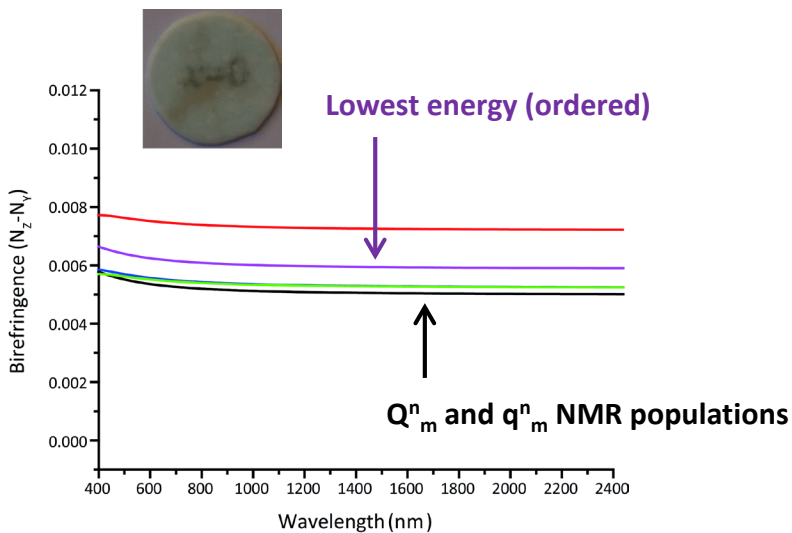→ **birefringence**

$$\Delta n = n_Z - n_Y$$
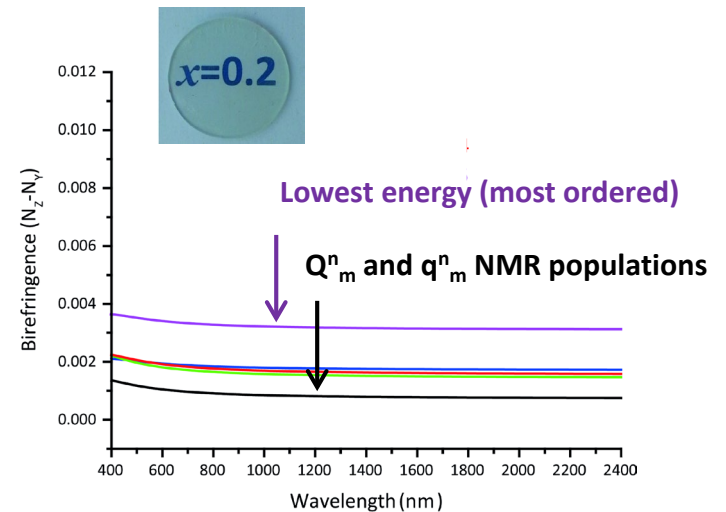
• *DFT*
• *PBE functional (GGA)*
• *ultrasoft pseudopotentials*

Calculation of refractive indexes with ~12% accuracy

Si/ Al disorder in tetrahedral sites

Si/ Al disorder in tetrahedral sites
Random partial occupancy of Sr2 site

Lowest energy (ordered)

Q^n_m and q^n_m NMR populations

x=0.2

Lowest energy (most ordered)

Q^n_m and q^n_m NMR populations

Variation of the birefringence as a function of the Al/Si ordering *(higher birefringence for full ordering)*

Chemical disorder → Tuning the birefringence of non-cubic crystalline phases

K. Al Saghir et al., *Chem. Mater.* 2015.

Conclusion

Structural description of (novel) materials

Diffraction
Synchrotron
Neutron
Electron

Microscopy
HR-TEM

Computations
Classical
DFT
AI/ML

Solid-State NMR
NMR crystallography approach

Make it **SMARTER….**

Acknowledgments

Orléans, France

NMR group

**Dominique Massiot, Pierre Florian,
Vincent Sarou-Kanian, Aydar Rakmatullin**,
Nadia Pellerin, Valérie Montouillout,
Michael Deschamps, Elodie Salager,
Catherine Bessada

CERAM group

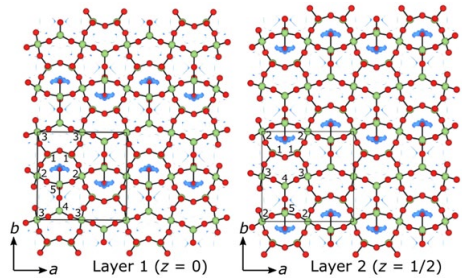Alberto Fernandez Carrion
Koloud Al Sagir,
Amandine Riouard

**Mathieu Allix,
Michael Pitcher
Cécile Genevois,
Emmanuel Véron,**

Thank you for your attention ;-)

Melilite compounds with extra oxide ions : $La_2Ga_3O_{7.5}$

Description of full chain ordering of O_{int} within the $[Ga_3O_{7.5}]$ layers

Layer 1 (z = 0)   Layer 2 (z = 1/2)

$[Ga_3O_7]$ framework along c
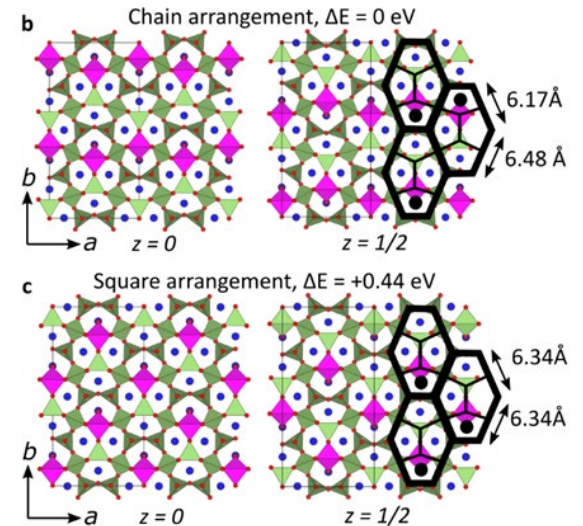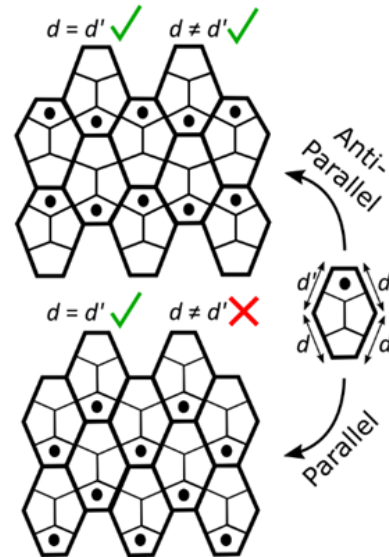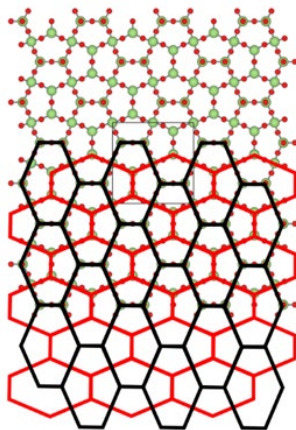→ *2 interpenetrating hexagonal networks*

M. Pitcher

Cemhti

Two possibilities: chains or squares arrangement of O_{int}

Antiparallel tiling
→ **No geometric constraint** on the tile
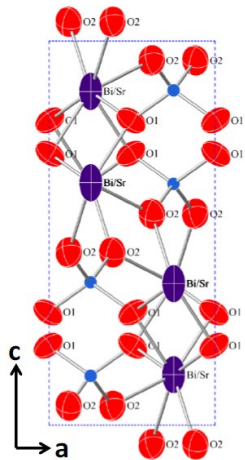→ chain arrangement *preferred*

Parallel tiling (square ordering)
→ **geometric constraint** on the tile ($d = d'$)
→ *loss of framework flexibility*
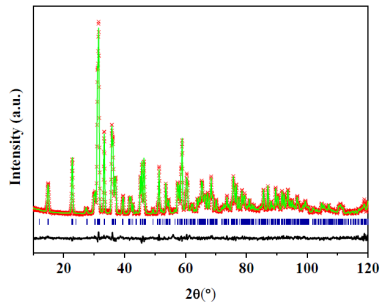
DFT geometry opt.

Chain arrangement, ΔE = 0 eV
6.17Å
6.48 Å
z = 0   z = 1/2

Square arrangement, ΔE = +0.44 eV
6.34Å
6.34Å
z = 0   z = 1/2

BiVO$_4$ and Bi$_{1-x}$Sr$_x$VO$_{4-x/2}$ Scheelite compounds

SPD & NPD

^{51}V NMR @ 20T

^{51}V frequency (ppm)

Average (long range) and local structure description
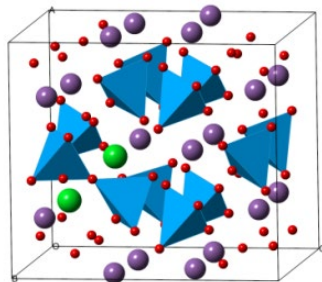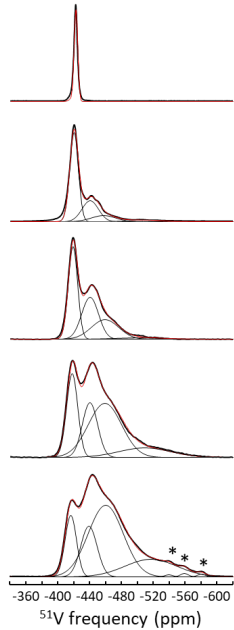
…SMARTER approach….

O vacancies migration mechanism
Molecular Dynamic simulations *(classical, DL-Poly)*

simulation box : **8 × 8 × 4** unit cells , **6112** atoms
Sr$_{0.0625}$Bi$_{0.9375}$VO$_{3.96875}$ composition
300 ps trajectory @ 1400K

MD trajectory @ 1400 K
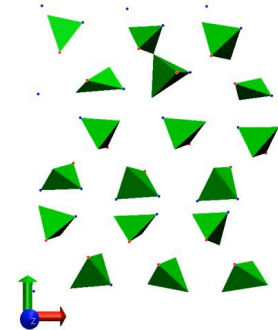
long-range migration of O vacancies
→ continuous breaking and reforming of V$_2$O$_7$

Ceramics : DFT computation of birefringence from models

• **Dielectric function**

$$\varepsilon(\omega) = \varepsilon_1(\omega) + i\,\varepsilon_2(\omega)$$

→ **refractive indexes**

$$n = \left(\frac{\sqrt{\varepsilon_1^2 + \varepsilon_2^2} + \varepsilon_1}{2} \right)^{1/2}$$

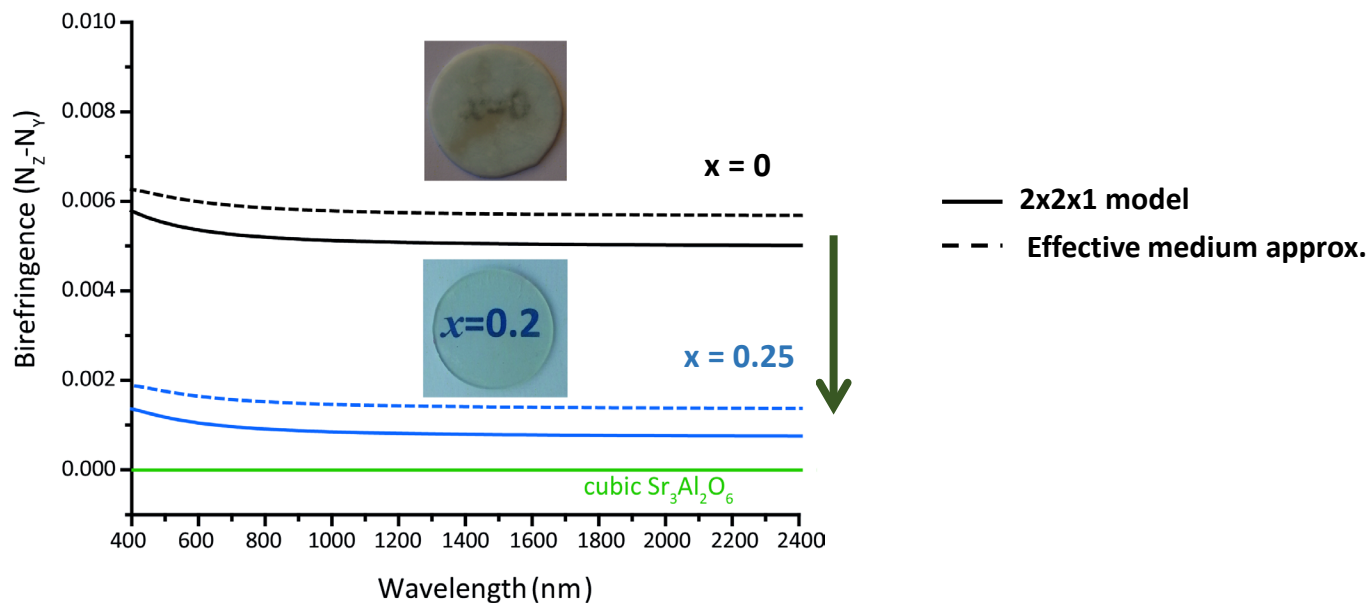→ **birefringence**

$$\Delta n = n_Z - n_Y$$

• *DFT*
• *PBE functional (GGA)*
• *ultrasoft pseudopotentials*

Calculation of refractive indexes with ~12% accuracy

Random partial occupancy of Sr2 site (Sr2 empty for x = 0)

Birefringence (N_Z-N_Y) vs Wavelength (nm)

x = 0
x = 0.2
x = 0.25
cubic $Sr_3Al_2O_6$

—— 2x2x1 model
– – Effective medium approx.

Decrease of the calculated birefringence for x = 0.25 in agreement with the **increase of the observed transparency**

K. Al Saghir, S. Chenu, E. Veron, F. Fayon, M. Suchomel, C. Genevois, F. Pocher, G. Matzen, D. Massiot, M. Allix, *Chem. Mater.* 2015.